EUROFUSION WPDIV-PR(15) 14248

M. Li et al.

Sweeping heat flux loads on divertor targets: thermal benefits and structural impacts

Preprint of Paper to be submitted for publication in
Fusion Engineering and Design

This work has been carried out within the framework of the EUROfusion Consortium and has received funding from the Euratom research and training programme 2014-2018 under grant agreement No 633053. The views and opinions expressed herein do not necessarily reflect those of the European Commission.

Sweeping heat flux loads on divertor targets: thermal benefits and structural impacts

Muyuan Li[a], Francesco Maviglia[b], Gianfranco Federici[b], Jeong-Ha You[a,*]

[a] *Max-Planck-Institut für Plasmaphysik, Boltzmannstr.2, 85748 Garching, Germany*
[b] *EUROfusion, PPPT, Boltzmann Str. 2, 85748 Garching, Germany*

Highlights

- Parametric simulations were carried out to study the impact of sweeping on thermo-mechanical response of a water-cooled divertor target .
- The maximum temperature and the heat flux to the coolant can be significantly reduced by sweeping.
- Sweeping gives benefits on fatigue lifetime as an emergency control action.
- Based on the fatigue lifetime prediction, sweeping is suitable for the stationary loading if the sweeping frequency is high enough.

Abstract

One possibility to mitigate the maximum high heat flux load on the target is to sweep the position of the strike-point back and forth periodically in order to spread the peak thermal load over a wider width. The aim of this work is to investigate the thermal and structure-mechanical responses of a water-cooled tungsten mono-block target under cyclic heat flux loads which are applied in sweeping modes. The study was performed by means of finite element analysis using an ITER-like target geometry. Extensive parametric simulations were carried out for a wide range of HHF loads and for two selected sweeping amplitudes and frequencies, respectively. The simulation shows that the maximum temperature and the heat flux to the coolant can be significantly reduced by sweeping. Sweeping gives benefits on fatigue lifetime of interlayer as an emergency control action. Based on the fatigue lifetime prediction of interlayer, sweeping is suitable for the stationary loading if the sweeping frequency is high enough.

*Corresponding author. Tel.: +49 (0)89 3299 1373; fax:+49 (0)89 3299 1212.
Email address: you@ipp.mpg.de (Jeong-Ha You)

keyword:. DEMO, divertor, LCF, strike-point sweeping

1. Introduction

In a tokamak-type fusion reactor, the high-energy plasma particles being detracted from the scrap-off layer onto the divertor target produce high heat flux (HHF)loads on the surface of the plasma facing target. The thermal loads are distributed highly heterogeneously over the poloidal positions of the target and locally concentrated around the strike-point which is the narrow intersection band of the separatrix with the target.

In the case of ITER divertor, the peak heat flux at the strike-point is predicted to reach $10\,\mathrm{MW/m^2}$ during stationary normal operation and even up to $20\,\mathrm{MW/m^2}$ during a slow transient event which lasts at least for a couple of seconds [1, 2]. For exhaustion of the thermal power, water-cooled tungsten monoblock target equipped with copper alloy tubes was employed for the ITER divertor. The recent HHF qualification tests conducted on the prototypes of ITER divertor target revealed that substantial damages were produced in the tungsten armor (deep cracks, melting) and in the cooling tube (plastic deformation), when the applied heat flux load approached $20\,\mathrm{MW/m^2}$ [3, 4]. This result raises a critical concern in terms of the structural integrity and reliability of the target components under transient thermal loads.

In the case of DEMO divertor target, the currently assumed HHF loads lie in the comparable range with those of the ITER divertor target. Therefore, the damage features mentioned above in relation to the ITER divertor target would still indicate critical design issues for the DEMO divertor target as well. Furthermore, the fracture failure risk of the armor, and potentially the tube as well, will become increasingly serious for the DEMO divertor target, as the neutron irradiation dose is expected to be at least an order of magnitude higher (3-6 dpa/fpy for the tungsten armor) than that of the ITER divertor target [5]. However, the technical feasibility to avoid or to mitigate the critical failure features seems to be quite limited. From the viewpoint of the current technological readiness, the metallurgical enhancement of the toughness of tungsten or copper alloy has been obviously stagnating. On the other hand, the safety margin of the target concept in terms of structural design criteria becomes highly tight, when the HHF load is increased toward $20\,\mathrm{MW/m^2}$. This trend is valid for the tungsten armor as well, although the armor is usually not regarded as actual structural part according to the conventional classification. Given such a highly demanding environment of structure-mechanical loading that is nearly approaching the performance limit, there arises a need to reduce and keep under control the peak thermal load down to a safe level.

One of the potential (maybe more fundamental) solutions would be to control in real time the radiative loss of fusion power (in excess of 90%) while maintaining the divertor plasma in a detached regime constantly.

However, the required technologies are by far distant from the engineering maturity. Even the underlying physics is only so little understood up to now that it will surely be a long-term mission. How robust and reliable this control technique will be able to be is another concern besides its basic feasibility. A possible failure of any controlling sequence is likely to cause a sudden increase of heat flux up to $20\,\mathrm{MW/m^2}$, where irreversible damage may be produced. When the loss-of-detachment event is continually repeated due to the misfunction of the control system, the accumulated damage may eventually result in the global failure of a whole component within an unacceptably short operation lifetime.

Another possibility to mitigate the maximum HHF load on the target is to sweep the position of the strike-point back and forth periodically in order to spread the peak thermal load over a wider width. The concept of strike-point sweeping has already been successfully implemented into the JET experiment campaigns [6, 7, 8]. It was applied to the divertor design of W7-X as well [9, 10]. A number of aspects need to be considered for evaluating the applicability of the sweeping concept [11]. For DEMO this technique could be applied either as an emergency control action, in case a sudden increase of the thermal load on the divertor target is detected, or as a steady state control scheme during normal operation. Extensive numerical estimations are being carried out to study the impact of various parameters on the thermal response of a target under sweeping operation, for instance, dimension of armor and heat sink, coolant inlet temperature, materials properties, and the time to coolant burn out. Additionally, to explore the feasibility of the sweeping technique for normal operation, comprehensive analyses are needed including required power, optimal amplitude and frequency of sweeping, impact on plasma shape and confinement quality, power dissipation due to the alternating currents induced in the neighboring superconductor coils and local temperature increase, and thermal fatigue of the materials due to the cyclic variation of thermal stresses.

The aim of this work is to investigate the thermal and structure-mechanical responses of a water-cooled tungsten mono-block target under cyclic heat flux loads which are applied in sweeping modes. The focus is on the quantitative assessment of thermal benefits, namely, the reduction of peak temperature and heat flux to the heat sink, and of structural risk caused by the thermal fatigue of the heat sink. The study was performed by means of finite element analysis using an ITER-like target geometry. Extensive parametric simulations were carried out for a wide range of HHF loads and for two selected sweeping amplitudes and frequencies, respectively. Obvious benefit of the sweeping scheme in thermal performance is demonstrated while the impact on the fatigue lifetime is addressed.

2. FE model

2.1. Geometry, FE mesh and materials

Fig. 1 shows the assumed footprint of the heat flux power on the outer target according to the latest prediction for DEMO based on [12]. The target consists of a number of small rectangular tungsten block connecting by a cooling tube. Two neighboring blocks are separated by a thin gap (∼0.3 mm). To study the influence of periodic strike point oscillation, the footprint of the heat flux power is swept at the surface of the targets along the axis direction of the cooling tube (x-axis), see Fig. 2. The heat flux profile along the y-axis is assumed to be constant. The control point of the sweeping is set to be the 0 width position in Fig. 1. The sweeping amplitude is defined as the distance between the rightmost and leftmost positions of the control point during sweeping. One mono-block divertor is selected for the thermal analysis in this work, and the rightmost position of the control point lies on the right edge of the top surface of the selected mono-block divertor. The position where the maximum temperature occurs during sweeping is dependent on the sweeping amplitude and the sweeping frequency. According to a rough estimation from a 2D finite element (FE) simulation, the difference between the maximum temperatures of the targets and of the selected mono-block divertor is less than 100°C for loading conditions studied in this work. For simplicity, the selected mono-block divertor is used for all the loading combinations.

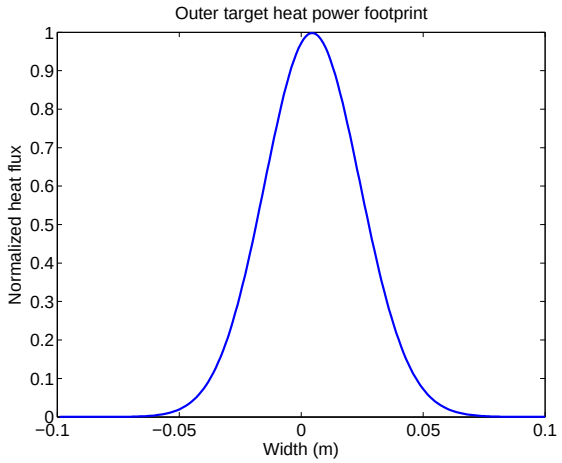

Fig. 1. The assumed footprint of the heat flux power on the outer target is according to the latest prediction for DEMO based on [12].

The PFC model considered for the FEM study is a water-cooled tungsten mono-block duplex structure consisting of a tungsten armor block and a copper alloy cooling tube (heat sink). The geometry, the FE mesh and the constituent materials of the considered model PFC are shown in Fig. 3. The tungsten armor block has dimensions of 23 × 22 × 4 mm. The cooling tube has a thickness of 1.0 mm and an inner diameter

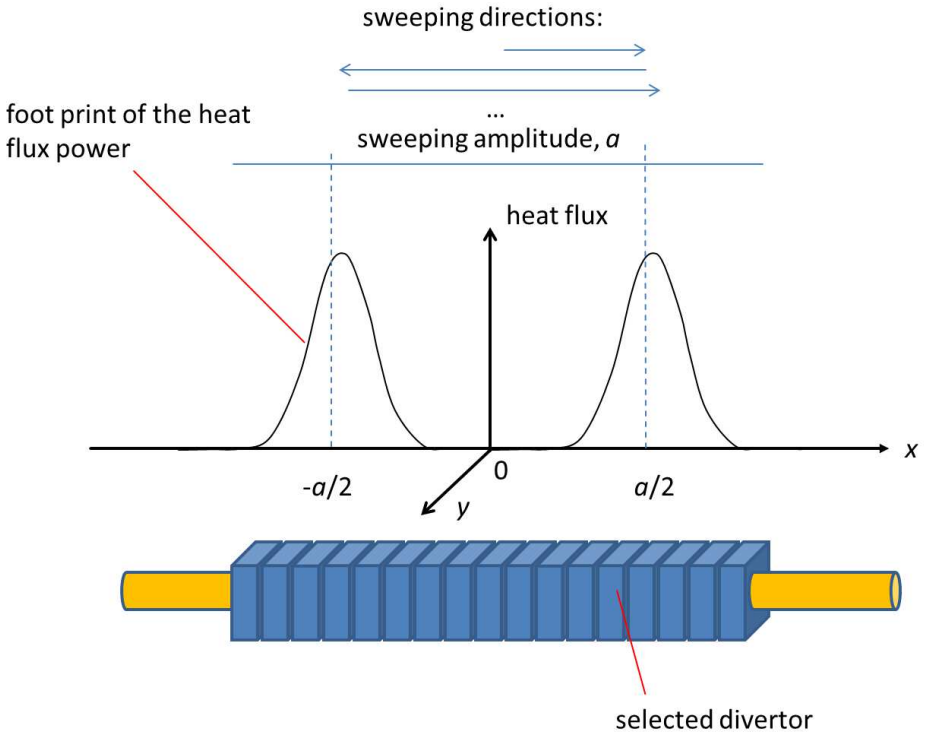

Fig. 2. Schematic drawing of sweeping the footprint of the heat flux power.

of 12 mm. The thickness of the copper interlayer is 0.5 mm. The geometry used here is based on the optimization of the geometry of the ITER tungsten divertor [13]. The commercial FEM code ABAQUS was employed for the numerical studies using quadratic brick elements of 20 nodes each. In total, there were 8496 finite elements. The mesh in the critical region of the component was refined.

At the selected mono-block divertor, the maximum temperature occurs at the left edge during sweeping. The nodes 1, 2 and 3 at the left edge are therefore selected to characterize the maximum temperatures in tungsten block, between tungsten and copper, and between copper alloy and coolant water for sweeping cases. The simulation for a stationary case is also performed as a reference. In the stationary case, the heat flux peak is positioned at the middle line between the left and right edges of the top surface. The nodes 4, 5 and 6 are used to characterize the maximum temperatures for the stationary case.

The thermo-mechanical simulations are based on data of several materials in the PFC model. Cross-rolled and stress-relieved tungsten was applied for the tungsten armor block. A precipitation-hardened copper alloy (CuCrZr) was considered for the heat sink tube and soft-annealed copper constituted the interlayer. The Frederick-Armstrong constitutive model applied for copper and the copper alloy is based on the combination of non-linear isotropic and kinematic hardening laws [14, 15, 16]. Temperature-dependent material properties

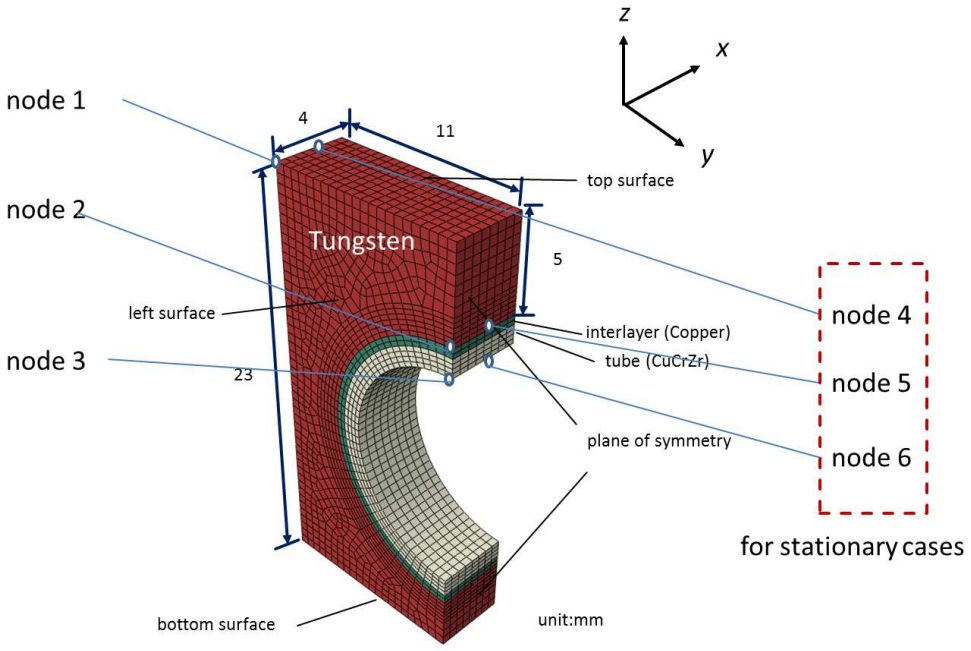

Fig. 3. The FE mesh of the mono-block divertor model. Due to symmetry only one half of the structure was considered.

are listed in Table 1 at selected temperatures, corresponding to the operation temperatures for the considered materials. It should be noted that the materials are assumed to be unirradiated due to lack of data of irradiated materials.

2.2. Loads and boundary conditions

The peak heat flux densities of 15 MW/m^2, 20 MW/m^2 and 30 MW/m^2 are applied in this study. Before the HHF load is applied, the PFC is assumed to have a uniform temperature (coolant temperature) without any residual stress. For a parametric study, the sweeping amplitudes of 5 cm and 20 cm are chosen. The sweeping frequency varies from 1 Hz to 0.5 Hz. Two further simulations that consider 10 MW/m^2 and 4 Hz are also performed to study the vadilty of applying sweeping as a steady state control scheme during normal operation.

The heat transfer coefficient between the inner wall of the heat sink tube and the coolant water is plotted in Fig. 4. It is calculated using SIEDER/TATE [19] and CEA/THOM [20] correlations for forced convection and subcooled boiling regimes, respectively. The pressure of the coolant water is 5 MPa. The coolant water velocity is 12 m/s. The temperature of the coolant water is 200°C. A swirl tape (thickness: 0.8 mm, twist ratio: 2) in the tube was assumed in the calculation of heat transfer coefficient.

Table 1. Properties of the considered materials at selected temperatures [17, 18].

	Tungsten[1]			CuCrZr[2]		Copper[3]	
	20 °C	400 °C	1200 °C	20 °C	400 °C	20 °C	400 °C
Young's modulus (GPa)	398	393	356	115	106	115	95
Yield stress (MPa)	1385	1100	346	273	238	3	3
Q^* (MPa)				-43	-68	76	36
b^*				6	10	8	25
C^* (MPa)				148575	117500	64257	31461
γ^*				930	1023	888	952
Heat conductivity (W/mK)	175	140	105	318	347	379	352
Coefficient of thermal expansion (10^{-6}/K)	4.5	4.6	5.3	16.7	17.8	17.8	18.1

[1] Rolled and stress-relieved state.
[2] Precipitation-hardened state, the reference alloy: Elmedur-X (code: CuCr1Zr, Cr: 0.8%, Zr: 0.08%).
[3] Softened by annealing at 700 °C for 1 h.
* Material parameters entering the Frederick-Armstrong constitutive model [18].

At two ends of the cooling tube, planar axial displacement constraint is given.

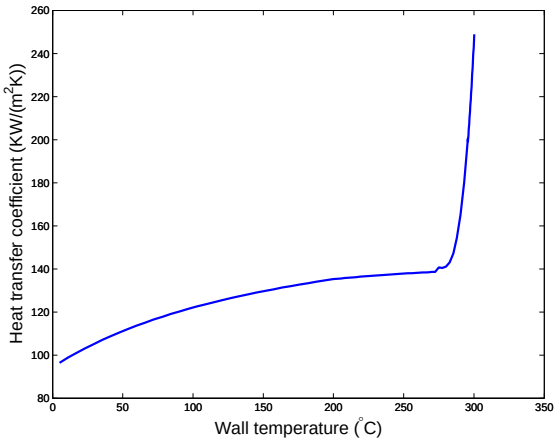

Fig. 4. Heat transfer coefficient between the inner wall of the heat sink tube and the coolant water. The coolant water velocity is 12 m/s. Pressure of the coolant water is 5 MPa. The temperature of the coolant water is 200°C. A swirl tape (thickness: 0.8 mm, twist ratio: 2) in the tube was assumed.

3. Results and discussion

3.1. Critical heat flux

The simulations were conducted with different sweeping frequencies and sweeping amplitudes. A higher sweeping frequency leads more thermal cycles within the same time but less loading time for each thermal cycle. Increasing the sweeping amplitude results in spreading the energy in a larger area, i.e. the energy input is reduced for each mono-block. Table 2 lists the heat flux densities at copper alloy-water interface (at node 3). The critical heat flux density is 25.29 MW/m^2 at wall temperature of 300°C for a coolant temperature of 200°C calculated using modified Tong 75 correlation according to the CEA formulation. When the heat flux to the coolant is above the critical value, the coolant loses heat removal capability. This effect is not included in the simulations. In the simulation, if the wall temperature is higher than 300°C, the maximum HTC in Fig. 4 will be applied. The maximum heat flux densities at copper alloy-water interface of stationary cases for 20 MW/m^2 and 30 MW/m^2 and sweeping cases with a sweeping amplitude of 5 cm for 30 MW/m^2 are much larger than the critical heat flux. Those results are unrealistic due to the inaccuracy of the HTC, and they are not listed here. For the stationary case of 15 MW/m^2, the heat flux is slightly above the critical value, but considering that this only occurs in the a limited area of the wall surface, the result is thought to be realistic in general.

When sweeping amplitude of 20 cm is applied, the heat flux density to the coolant can be reduced below the critical value. For the best combination of sweeping amplitude and frequency (20 cm and 1 Hz) listed in Table 2, the heat flux density to the coolant can be reduced as a factor of 4. Furthermore, as the loading

time on one mono-block divertor is significantly reduced by sweeping, the damage induced by a sudden increase of the heat flux density will be smaller than that in the stationary cases.

Table 2. Maximum heat flux density (MW/m^2) [temperature ($^\circ C$)] at copper alloy-water interface (at node 3).

Peak heat flux density (MW/m^2)	15		20		30	
Sweeping frequency (Hz)	0.5	1	0.5	1	0.5	1
Sweeping amplitude (cm)						
5	20.6 (297)	18.2 (295)	-	24.8 (300)	-	-
20	8.6 (262)	6.0 (243)	11.3 (280)	7.8 (257)	19.0 (295)	11.6 (281)
Stationary case	25.4 (302)		-		-	

– critical heat flux is reached.

3.2. Temperature

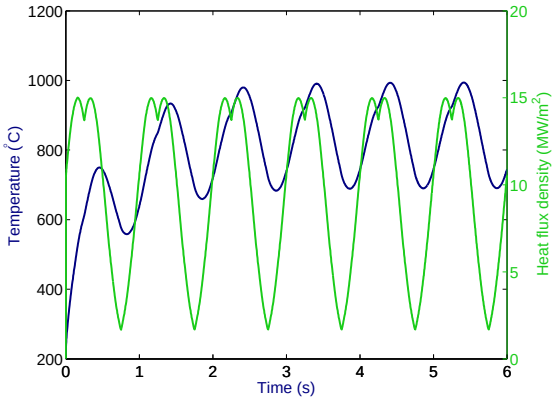

Fig. 5. Temperature and heat flux density at node 1 as a function of time for peak heat flux density of 15 MW/m^2 with sweeping frequency of 1 Hz and sweeping amplitude of 5 cm.

Fig. 5 shows temperature and heat flux density at node 1 as a function of time for peak heat flux density of 15 MW/m^2 with sweeping frequency of 1 Hz and sweeping amplitude of 5 cm. Two peaks of heat flux density at node 1 in one thermal cycle are quite close to each other, since the selected mono-block is located near the edge of the sweeping area. The peak temperature occurs shortly after the occurrence of the second peak of the heat flux density. After a few seconds, a saturating thermal cycle is observed.

Fig. 6 shows the temperature at node 1 for peak heat flux densities of 15 MW/m^2, 20 MW/m^2 and 30 MW/m^2. The temperature is much higher for a sweeping amplitude of 5 cm than 20 cm. When the sweeping frequency increases, the peak temperature decreases. As a result, the peak temperature at the top surface of the mono-block can be reduced by increasing either the sweeping amplitude or the sweeping frequency. However, the increasing the sweeping amplitude will be limited by the geometry of divertor target. A higher sweeping frequency will require more thermal cycles during the operation, but at the same

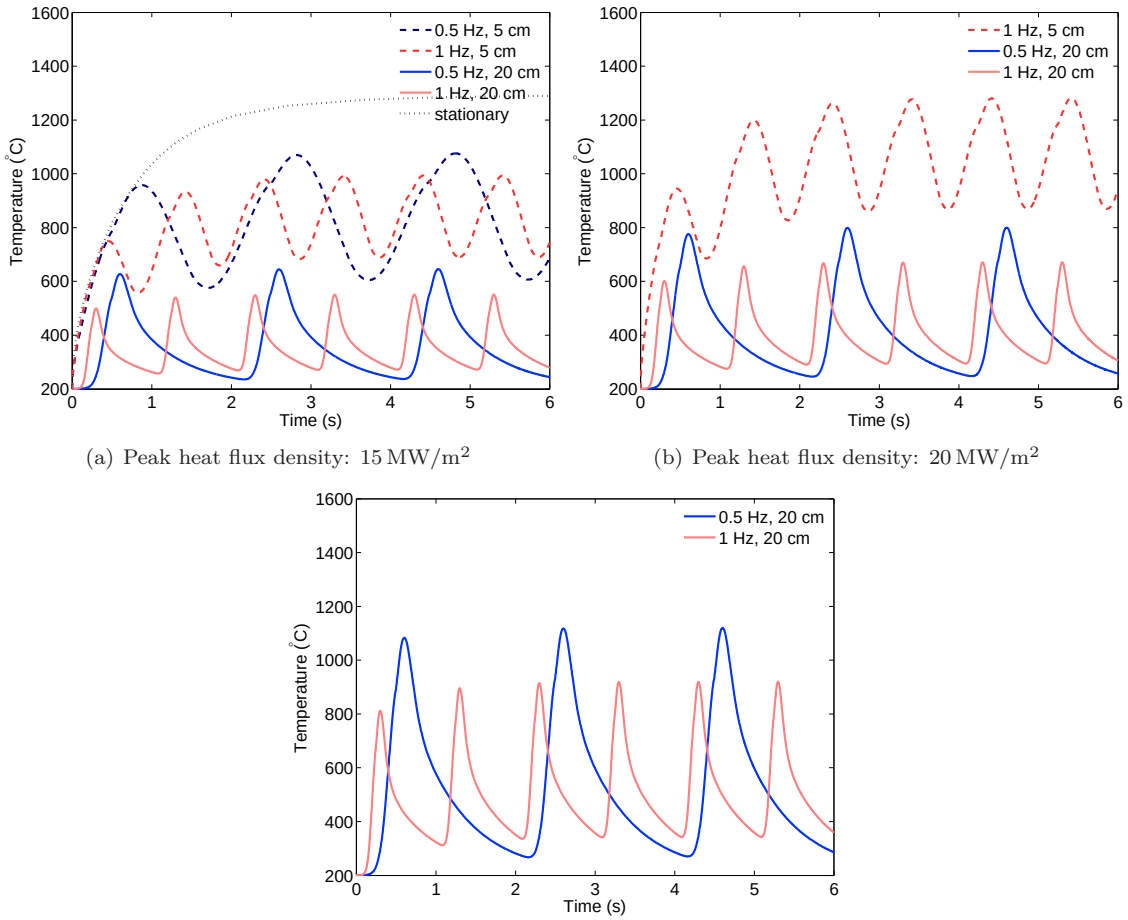

(a) Peak heat flux density: 15 MW/m^2

(b) Peak heat flux density: 20 MW/m^2

(c) Peak heat flux density: 30 MW/m^2

Fig. 6. Temperature at node 1 as a function of time for different peak heat flux densities.

time, it reduces the temperature variation as well as the loading time in each thermal cycle. The former will certainly shorten the actual operating time but the later will enlarge the allowed number of load cycles (fatigue lifetime). The study of impact of increasing sweeping frequency on LCF behavior will be shown later in this section.

Table 3 gives maximum and minimum temperatures at node 1 in the saturating thermal cycle. When the sweeping frequency increases from 0.5 to 1 Hz, the maximum temperature decreases and the minimum temperature increases. As a result, the temperature amplitudes drop more than 30%. When the sweeping amplitude of 20 cm is applied instead of 5 cm, both the maximum and the minimum temperatures decrease, and the reduction in the temperature variation amplitude is less than 15%, which deceases with increasing the frequency. For the peak heat flux density of 20 MW/m^2 (1 Hz and 5 cm) and 30 MW/m^2 (0.5 Hz and 20 cm), the maximum temperatures enter the crystallization temperature range of tungsten (1100-1400°C).

Table 3. Maximum / Minimum (amplitude) temperatures (°C) at node 1 in the saturating thermal cycle.

Sweeping amplitude (cm)	5		20	
Sweeping frequency (Hz)	0.5	1	0.5	1
Peak heat flux density (MW/m^2)				
15	1076/606 (470)	993/698 (295)	645/244 (401)	551/271 (280)
Maximum temperature (stationary)		1291		
20	-	1281/896 (385)	800/247 (553)	671/294 (377)
Maximum temperature (stationary)		-		
30	-	-	1119/286 (833)	920/342 (578)
Maximum temperature (stationary)		-		

– critical heat flux is reached.

When tungsten at the surface layer is recrystallized, the strength of tungsten is significantly reduced, and major cracks have been observed in the heat flux tests of divertors [3]. When there is no recrystallized layer at the surface, the brittle cracking is not critical in the tungsten armor block [21].

Table 4. Maximum / Minimum (amplitude) temperatures (°C) at node 2 in the saturating thermal cycle.

Sweeping amplitude (cm)	5		20	
Sweeping frequency (Hz)	0.5	1	0.5	1
Peak heat flux density (MW/m^2)				
15	378/306 (72)	367/328 (39)	297/216 (81)	268/223 (45)
Maximum temperature (stationary)		401		
20	-	398/355 (43)	327/215 (112)	288/230 (58)
Maximum temperature (stationary)		-		
30	-	-	370/230 (140)	328/245 (83)
Maximum temperature (stationary)		-		

– critical heat flux is reached.

Fig. 7 shows the temperature at node 2 for peak heat flux densities of 15 MW/m^2, 20 MW/m^2 and 30 MW/m^2. The impact of the sweeping amplitude and the sweeping frequency on the temperature is similar. The maximum temperature in the saturating thermal cycle can be reduced to below 400°C by applying a sweeping amplitude of 20 cm for the peak heat flux density of up to 30 MW/m^2. The high temperature (above 400°C) is critical at the interface between tungsten armor block and copper interlayer, as the copper will become softer. Maximum and minimum temperatures at node 2 are listed in Table 4. Compared to the situation at the top surface, the temperature variation at node 2 is less significant and its amplitude is less than 20% of that at node 1. However, the temperature variation in the copper interlayer is more critical, since a large amount of plastic deformation will be generated due to the temperature variation leading to LCF failure [22]. Different from the trend of maximum at the top surface, the temperature amplitude increases, if the sweeping amplitude increase from 5 cm to 20 cm. This is because for the sweeping amplitude of 20 cm, the selected mono-block can be more sufficiently cooled.

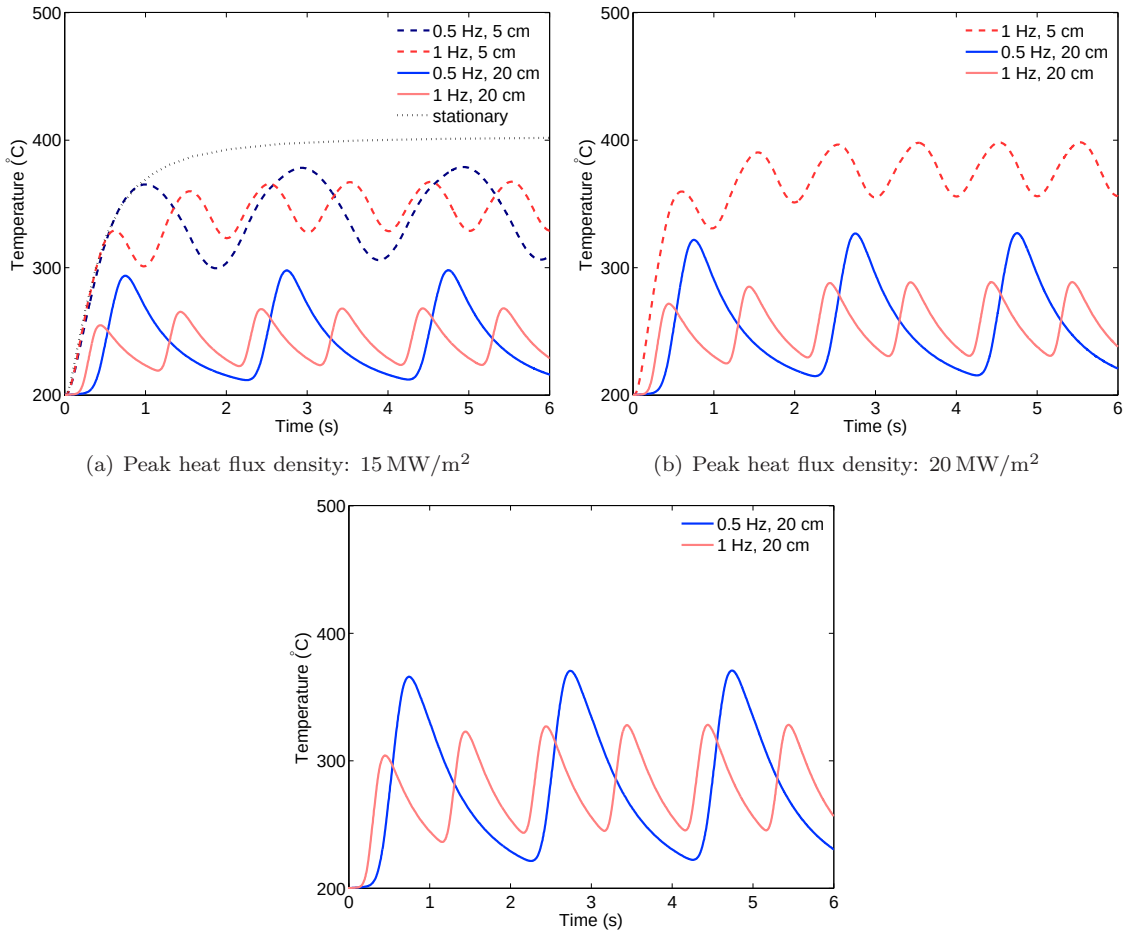

(a) Peak heat flux density: 15 MW/m^2

(b) Peak heat flux density: 20 MW/m^2

(c) Peak heat flux density: 30 MW/m^2

Fig. 7. Temperature at node 2 as a function of time.

3.3. Fatigue lifetime

As shown in the previous study [22], significant plastic deformation accumulation occurs in the interlayer, while nearly no cyclic plastic deformation is accumulated in the cooling tube. Thus, in this work, we focus on the impact of sweeping parameters on the accumulated equivalent plastic strain in the copper interlayer (the reference node is chosen in the middle of the interlayer at the plane of symmetry representing a most general case). Fig. 8 shows accumulated equivalent plastic strain in the copper interlayer. The accumulated equivalent plastic strains increase as the peak heat flux densities increase. Table 5 lists the predicted equivalent plastic range at the last thermal cycle as well as the fatigue lifetime of the interlayer. One can find more details of fatigue lifetime calculations in the previous study [22].

The fatigue lifetime increases as the peak flux densities decrease. A greater fatigue lifetime is predicted if

the sweeping amplitude decreases from 20 cm to 5 cm. If the sweeping frequency is doubled (from 0.5 Hz to 1 Hz), the fatigue lifetime is increased at least by a factor of 4. As a result, increasing the sweeping frequency from 0.5 Hz to 1 Hz will increase the actual operating time for interlayer. Assuming the loading duration (pulse time) for a quasi-stationary case is 10 s (e.g. the slow transient case), when sweeping frequency of 1 Hz is applied, the number of load cycles is at least 10 times larger than that for stationary loading in the same operating time. For 0.5 Hz, it is at least 5 times larger. Converting the fatigue lifetime to the number of pulses of 10 s, for the peak heat flux density of 15 MW/m^2 (20 cm) sweeping the HHF load (15286 pulses) gives benefits for actual operating time compared to the non-sweeping stationary case (12553 pulses). However, when the pulse time is assumed to be 7200 s (e.g. the stationary case in DEMO, [23]), it will result in a much shorter actual operating time. E.g., for peak heat flux density of 15 MW/m^2 with 0.5 Hz and 20 cm, converting the fatigue lifetime to the number of pulses of 7200 s, the interlayer will fail after 21 pulses compared to 12553 pulses for non-sweeping case. With above mentioned parameters, sweeping can be applied as an emergency control action, in case a sudden increase of the thermal load on the divertor target is detected.

Two further sweeping simulations for the peak heat flux density of 10 MW/m^2 (1 Hz and 20 cm) and the peak heat flux density of 15 MW/m^2 (4 Hz and 20 cm) are performed for studying the stationary case in ITER and DEMO. The predicted fatigue lifetime for the peak heat flux density of 10 MW/m^2 (1 Hz and 20 cm) is 1133500 cycles, which is 157 pulses by converting the fatigue lifetime to the number of pulses of 7200 s. However, when the sweeping frequency is increased to 4 Hz, the predicted fatigue lifetime for 15 MW/m^2 with 20 cm is 1.99×10^8 cycles, which is 6906 pulses. Although it is still 4 times less than the non-sweeping case (29991 pulses), it increases dramatically compared to the sweeping case with 0.5 Hz. In this sense, sweeping can be applied as a steady state control scheme during normal operation with a frequency which is high enough.

One needs to be noted that, the sweeping the HHF load in a larger area reduces the loading time for each divertor, which is an advantage for minimizing the thermal-induced material degradation (e.g. recrystallization) and the possible creep effect.

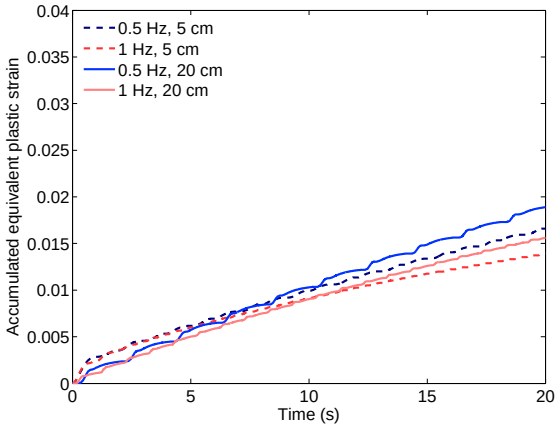

(a) Peak heat flux density: 15 MW/m^2

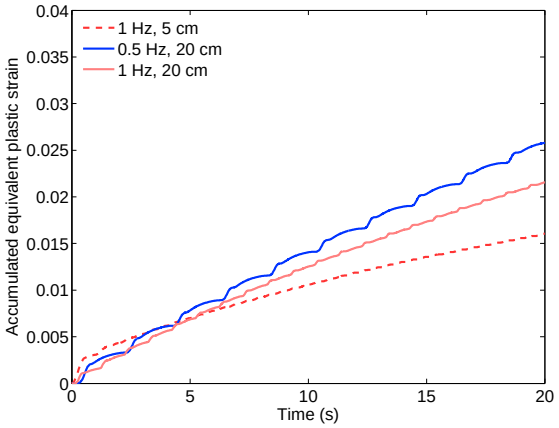

(b) Peak heat flux density: 20 MW/m^2

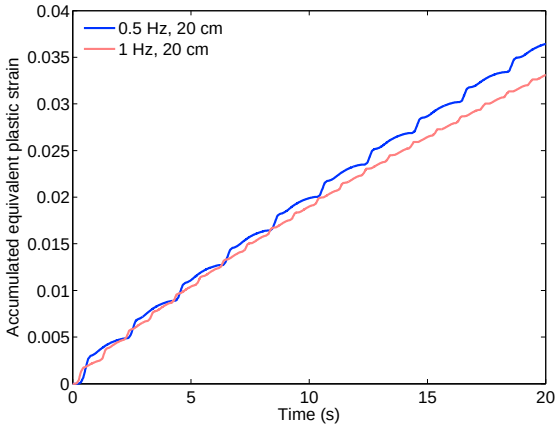

(c) Peak heat flux density: 30 MW/m^2

Fig. 8. Accumulated equivalent plastic strain in the copper interlayer.

Table 5. Predicted equivalent plastic strain range (%) / fatigue lifetime[a] in the copper interlayer.

Peak heat flux density (MW/m^2)	15		20	
Sweeping frequency (Hz)	0.5	1	0.5	1
Sweeping amplitude (cm)				
5	0.064/119950	0.021/852700	-	0.023/677900
20	0.082/76430	0.029/482960	0.112/44050	0.040/271090
Peak heat flux density (MW/m^2)	30			
Sweeping frequency (Hz)	0.5	1		
Sweeping amplitude (cm)				
5	-	-		
20	0.159/24043	0.064/118300		
Peak heat flux density (MW/m^2)	10		15	
Stationary case [22]	0.14/29991		0.23/12553	

[a] Fatigue lifetime (allowed number of load cycles) was estimated from the reported fatigue data using plastic strain for unirradiated copper in the ITER Material Properties Handbook [24].
– critical heat flux is reached.

4. Summary and conclusions

In this paper, the results of an extensive computational study was reported which was carried out to assess the basic feasibility of the divertor heat flux sweeping technique in terms of the thermal and structural performance of a water-cooled tungsten mono-block target. Parametric finite element simulations demonstrated a significant thermal benefit of sweeping to reduce the peak temperature on the target. The increased number of temperature fluctuation cycles was shown to cause a trade-off effect affecting the structure-mechanical performance due to accelerated plastic fatigue. The sweeping amplitude and frequency turned out to have a considerable impact on the thermal efficiency of sweeping operation. The major predictions are summarized as follows:

1. The peak temperature decreases, when the sweeping amplitude or the sweeping frequency increases. The peak heat flux to the coolant is significantly reduced by sweeping as well.
2. With an optimal combination of sweeping amplitude and frequency, even the extreme heat flux load of $30\,\mathrm{MW/m^2}$ could be accommodated without exceeding critical heat flux or armor melting point.
3. The increase of sweeping frequency (from 0.5 to 1 Hz) or decrease of sweeping amplitude (from 20 to 5 cm) has a beneficial effect on fatigue lifetime of the interlayer.
4. Sweeping gives benefits on fatigue lifetime of interlayer as an emergency control action, in case a sudden increase of the thermal load on the divertor target is detected.
5. Sweeping seems to be suitable for the stationary loading if the sweeping frequency is high enough.

Acknowledgement

The authors are grateful to Dr. Fabio Crescenzi at ENEA for his providing us the data of heat transfer coefficient and critical heat flux. This work has been carried out within the framework of the EUROfusion Consortium and has received funding from the European Union's Horizon 2020 research and innovation programme under grant agreement number 633053. The views and opinions expressed herein do not necessarily reflect those of the European Commission.

References

[1] M. Merola, D. Loesser, A. Martin, P. Chappuis, R. Mitteau, V. Komarov, R. Pitts, S. Gicquel, V. Barabash, L. Giancarli, J. Palmer, M. Nakahira, A. Loarte, D. Campbell, R. Eaton, A. Kukushkin, M. Sugihara, F. Zhang, C. Kim, R. Raffray, L. Ferrand, D. Yao, S. Sadakov, A. Furmanek, V. Rozov, T. Hirai, F. Escourbiac, T. Jokinen, B. Calcagno, S. Mori, ITER plasma-facing components, Fusion Engineering and Design 85 (2010) 2312–2322.

[2] A. Raffray, R. Nygren, D. Whyte, S. Abdel-Khalik, R. Doerner, F. Escourbiac, T. Evans, R. Goldston, D. Hoelzer, S. Konishi, P. Lorenzetto, M. Merola, R. Neu, P. Norajitra, R. Pitts, M. Rieth, M. Roedig, T. Rognlien, S. Suzuki, M. Tillack, C. Wong, High heat flux components - readiness to proceed from near term fusion systems to power plants, Fusion Engineering and Design 85 (2010) 93–108.

[3] G. Pintsuk, I. Bobin-Vastra, S. Constans, P. Gavila, M. Rödig, B. Riccardi, Qualification and post-mortem characterization of tungsten mock-ups exposed to cyclic high heat flux loading, Fusion Engineering and Design 88 (2013) 1858 – 1861.

[4] G. Pintsuk, M. Bednarek, P. Gavila, S. Gerzoskovitz, J. Linke, P. Lorenzetto, B. Riccardi, F. Escourbiac, Characterization of ITER tungsten qualification mock-ups exposed to high cyclic thermal loads, Fusion Engineering and Designdoi:http://dx.doi.org/10.1016/j.fusengdes.2015.01.037.

[5] J. H. You, A review on two previous divertor target concepts for DEMO: Mutual impact between structural design requirements and materials performance, Nuclear Fusion, submitted.

[6] E. Bertolini, Impact of JET experimental results and engineering development on the definition of the ITER design concept, Fusion Engineering and Design 27 (1995) 27 – 38.

[7] R. Albanese, G. Ambrosino, M. Ariola, A. Cenedese, F. Crisanti, G. D. Tommasi, M. Mattei, F. Piccolo, A. Pironti, F. Sartori, F. Villone, Design, implementation and test of the XSC extreme shape controller in JET, Fusion Engineering and Design 74 (2005) 627 – 632.

[8] G. Ambrosino, M. Ariola, G. De Tommasi, A. Pironti, F. Sartori, E. Joffrin, F. Villone, Plasma strike-point sweeping on jet tokamak with the extreme shape controller, Plasma Science, IEEE Transactions on 36 (2008) 834–840.

[9] R. Koenig, P. Grigull, K. McCormick, Y. Feng, J. Kisslinger, A. Komori, S. Masuzaki, K. Matsuoka, T. Obiki, N. Ohyabu, H. Renner, F. Sardei, F. Wagner, A. Werner, The divertor program in stellarators, Plasma Physics and Controlled Fusion 44 (2002) 2365.

[10] H. Renner, J. Boscary, H. Greuner, H. Grote, F. W. Hoffmann, J. Kisslinger, E. Strumberger, B. Mendelevitch, Divertor concept for the w7-x stellarator and mode of operation, Plasma Physics and Controlled Fusion 44 (2002) 1005.

[11] F. Maviglia, G. Federici, G. Strohmayer, R. Wenninger, C. Bachmann, R. Albanese, R. Ambrosino, M. Li, V. Loschiavo, J. You, L. Zani., Limitations of Transient Power Loads on DEMO and Analysis of Mitigation Techniques, 12th International Symposium on Fusion Nuclear Technology, Jeju, Korea, 2015 (accepted).

[12] T. Eich, A. Leonard, R. Pitts, W. Fundamenski, R. Goldston, T. Gray, A. Herrmann, A. Kirk, A. Kallenbach, O. Kardaun, A. Kukushkin, B. LaBombard, R. Maingi, M. Makowski, A. Scarabosio, B. Sieglin, J. Terry, A. Thornton, A. U. Team, J. E. Contributors, Scaling of the tokamak near the scrape-off layer h-mode power width and implications for ITER, Nuclear Fusion 53 (2013) 093031.

[13] F. Crescenzi, A. Moriani, S. Roccella, E. Visca, M. Richou, Water-cooled divertor target design study CuCrZr/W monoblock concept, EFDA report: WP13-DAS02-T02-D02 (2013).

[14] J. Lemaitre, J.-L. Chaboche, Mechanics of Solid Materials, 1st Edition, Cambridge University Press, 1994.

[15] P. J. Armstrong, C. O. Frederick, A mathematical representation of the multiaxial Bauschinger effect, G.E.G.B. Report RD/B/N (1966) 731.

[16] J. Chaboche, Constitutive equations for cyclic plasticity and cyclic viscoplasticity, International Journal of Plasticity 5 (1989) 247–302.

[17] ITER structural design criteria for in-vessel components (SDC-IC) appendix A:Materials design limit data, ITER, (2001).

[18] J.-H. You, M. Miskiewicz, Material parameters of copper and CuCrZr alloy for cyclic plasticity at elevated temperatures, Journal of Nuclear Materials 373 (2008) 269–274.

[19] E. N. Sieder, G. E. Tate, Heat transfer and pressure drop of liquids in tubes, Industrial & Engineering Chemistry 28

(1936) 1429–1435.

[20] J. Thom, W. Walker, T. Fallon, G. Reising, Boiling in sub-cooled water during flow up heated tubes or annuli., Proc. Inst. Mech. Eng. (London), 180: Pt 3C, 226-46(1965-66).

[21] M. Li, E. Werner, J.-H. You, Fracture mechanical analysis of tungsten armor failure of a water-cooled divertor target, Fusion Engineering and Design 89 (2014) 2716–2725.

[22] M. Li, E. Werner, J.-H. You, Low cycle fatigue behavior of iter-like divertor target under demo-relevant operation conditions, Fusion Engineering and Design 90 (2015) 88–96.

[23] G. Giruzzi, J. Artaud, M. Baruzzo, T. Bolzonella, E. Fable, L. Garzotti, I. Ivanova-Stanik, R. Kemp, D. King, M. Schneider, R. Stankiewicz, W. Stępniewski, P. Vincenzi, D. Ward, R. Zagórski, Modelling of pulsed and steady-state DEMO scenarios, Nuclear Fusion 55 (2015) 073002.

[24] ITER Material Properties Handbook, ITER Document No.G74 MA 16, 2005.